

Supplement of Atmos. Chem. Phys., 15, 5275–5303, 2015  
<http://www.atmos-chem-phys.net/15/5275/2015/>  
doi:10.5194/acp-15-5275-2015-supplement  
© Author(s) 2015. CC Attribution 3.0 License.



*Supplement of*

## **Data assimilation of satellite-retrieved ozone, carbon monoxide and nitrogen dioxide with ECMWF's Composition-IFS**

**A. Inness et al.**

*Correspondence to:* A. Inness (a.inness@ecmwf.int)

The copyright of individual parts of the supplement might differ from the CC-BY 3.0 licence.

## 1 **1 Validation datasets**

2 Tropospheric CO data from the experiments are validated with profiles from the MOZAIC  
3 (Measurement of Ozone, Water Vapour, Carbon Monoxide and Nitrogen Oxides by Airbus In-  
4 service Aircraft) programme (Marenco et al., 1998; Nedelec et al., 2003) taken during aircraft  
5 ascents and descents at various airports. The MOZAIC CO analyser is based on the Gas Filter  
6 Correlation principle of infrared absorption by the 4.67  $\mu\text{m}$  CO band. The MOZAIC CO data  
7 have a total uncertainty of  $\pm 5$  parts per billion volume (ppbv), a precision of  $\pm 5$  %, and a  
8 detection limit of 10 ppbv (Nedelec et al., 2003). We use MOZAIC profiles from Frankfurt  
9 (837 profiles) and Windhoek (323 profiles).

10 Tropospheric CO profiles and columns are further validated against Network for the Detection  
11 of Atmospheric Composition Change (NDACC) ground-based Fourier Transform Infrared  
12 spectrometer (FTIR) measurements (see <http://ndacc.org>). The NDACC FTIR data are acquired  
13 according to formal measurement protocols, ensuring their traceability. The median random  
14 uncertainty of the FTIR data is 2-5 % for tropospheric columns and about 10-25 % at individual  
15 profile levels. They have the largest sensitivity in the mid and upper troposphere (and in the  
16 lower stratosphere which is not evaluated here). The model profiles are smoothed with the  
17 FTIR vertical averaging kernels and a-priori profile using the Rodgers formula (Rodgers, 2000).  
18 For column comparisons, the model tropospheric vertical column between the NDACC station  
19 altitude and 10 km in molecules/cm<sup>2</sup> is obtained by integrating the smoothed model volume  
20 mixing ratio (VMR) profile over the pressure differences. The methodology was developed in  
21 the EU FP7 project NORS (Demonstration Network Of ground-based Remote Sensing  
22 Observations in support of the Copernicus Atmospheric Service, [nors.aeronomie.be](http://nors.aeronomie.be)) and relies  
23 on validation methods described in Dils et al. (2006) and de Laat et al. (2010). The NORS co-  
24 location and smoothing algorithms are described by Langerock et al. (2014). A list of the  
25 selected NDACC FTIR stations is shown in Table S2.

26 Surface O<sub>3</sub> and CO mixing ratios are compared against WMO Global Atmosphere Watch  
27 (GAW) observations at selected background stations (e.g., Oltmans and Levy, 1994; Novelli  
28 and Masarie, 2014). The GAW observations represent the global background away from the  
29 main polluted areas. Detailed information on GAW and GAW related O<sub>3</sub> and CO measurements  
30 can be found in GAW reports No. 209 (2013) and No. 192 (2010) respectively  
31 ([http://www.wmo.int/pages/prog/arep/gaw/gaw\\_home\\_en.html](http://www.wmo.int/pages/prog/arep/gaw/gaw_home_en.html)). For detection of long-term  
32 trends and year-to-year variability, the data quality objectives (DQOs) for CO in GAW

1 measurements can reach a maximum uncertainty between  $\pm 2$  ppbv and  $\pm 5$  ppbv for marine  
 2 boundary layer sites and continental sites that are influenced by regional pollution (WMO  
 3 (2010). For surface ozone an average uncertainty of  $\pm 1$  ppbv is quoted in WMO (2013). The  
 4 stations used for the CO validations are listed in Table S3. The CO model values are  
 5 interpolated in time to the instantaneous measurements and then averaged on a monthly basis.  
 6 The procedure described in Flemming et al. (2009b) is applied to determine the model level  
 7 used to compare the model field with GAW surface observations. This method is based on the  
 8 difference between a high resolution orography and the actual station height. For O<sub>3</sub> 3-hourly  
 9 surface observations at 60 GAW stations (see Table S4) are used to calculate modified  
 10 normalized mean biases (MNMB) and correlation coefficients from daily mean values. The  
 11 MNMB is defined as

$$12 \quad MNMB = \frac{2}{N} \sum_{i=1}^N \frac{m_i - o_i}{m_i + o_i} \quad (1)$$

13 and the correlation coefficient as

$$14 \quad R = \frac{\frac{1}{N} \sum_{i=1}^N (m_i - \bar{m})(o_i - \bar{o})}{\sigma_m \sigma_o} \quad (2)$$

15 with N the number of observations, m the model and o the observed values,  $\bar{m}$  and  $\bar{o}$  the mean  
 16 values of model and observed values and  $\sigma_m$  and  $\sigma_o$  the corresponding SDs. Total column O<sub>3</sub>  
 17 (TCO<sub>3</sub>) is validated against KNMI's multi sensor reanalysis (MSR, van der A et al., 2010)  
 18 which is based on SBUV/2, GOME, TOMS, SCIAMACHY and OMI observations. All satellite  
 19 retrieval products as used in the MSR were bias-corrected with respect to Brewer and Dobson  
 20 Spectrophotometers to remove discrepancies between the different satellite data sets. The  
 21 uncertainty in the product, as quantified by the bias of the observation-minus-analysis statistics,  
 22 is of the order of 1 DU (van der A et al., 2010).

23 Stratospheric ozone fields are validated with version 3.0 retrievals of the Atmospheric  
 24 Chemistry Experiment Fourier Transform Spectrometer (ACE-FTS, Dupuy et al., 2009), which  
 25 observes the limb using the solar occultation technique, delivering up to 24 profiles per day.  
 26 The previous version of these retrievals (V2.2) was extensively validated against 11 other  
 27 satellite instruments, ozonesondes and several types of ground-based instruments (Dupuy et al.,  
 28 2009). This validation found a slight positive bias with mean relative differences of about 5%  
 29 between 15 and 45 km and reported that with version 3.0 this slight positive bias in the

1 stratosphere had been removed. With respect to precision, the same study found that the de-  
2 biased standard deviation of the mean relative differences between ACE-FTS V2.2 and  
3 ozonesondes fell within 12 to 15% (17 to 30%) above (below) 20 km.

4 We use for further validation the MIPAS ozone profiles retrieved by version 6 of the operational  
5 ESA processor (Raspollini et al., 2013). MIPAS is a limb-viewing high-resolution Fourier-  
6 transform spectrometer that measured atmospheric emissions in the near to mid-infrared part  
7 of the spectrum (4.15 microns to 14.6 microns), allowing the retrieval of concentration profiles  
8 of O<sub>3</sub> and other trace gases between about 0.1 to 200 hPa. The random and systematic errors  
9 for O<sub>3</sub> are between 5 and 10% for large parts of the profiles, but larger near the boundaries of  
10 the retrieval range. Even though MIPAS profiles are assimilated in CIFS-AN and therefore not  
11 an independent data set, they are used for validation too, because the good consistency between  
12 the ACE and MIPAS data give extra credibility to the validation results.

13 Ozonesondes are used to validate stratospheric and tropospheric ozone from the experiments.  
14 The ozonesonde data used for the validation are acquired according to WMO-recommended  
15 standard operation procedures (SOP) and archived in a variety of data centres: World Ozone  
16 and ULTaviolet Radiation Data Centre (WOUDC), Southern Hemisphere ADDitional  
17 OZonesondes (SHADOZ), Network for the Detection of Atmospheric Composition Change  
18 (NDACC), and campaigns for the Determination of Stratospheric Polar Ozone Losses  
19 (MATCH). The precision of electrochemical concentration cell (ECC) ozonesondes is on the  
20 order of  $\pm 5\%$  in the range between 200 and 10 hPa, between  $-14\%$  and  $+6\%$  above 10 hPa, and  
21 between  $-7\%$  and  $+17\%$  below 200 hPa (Komhyr et al., 1995). Larger errors are found in the  
22 presence of steep gradients and where the ozone amount is low. The same order of precision  
23 was found by Steinbrecht et al. (1998) for Brewer–Mast sondes. We average the available  
24 sondes in the areas: Arctic, North America, Europe, East Asia, Tropics, Antarctica (see Table  
25 S5 for more details about the sonde locations and numbers).

26 Tropospheric column NO<sub>2</sub> (TRCNO<sub>2</sub>) data from the experiments are compared with data  
27 retrieved from the GOME-2 instrument which measures in the ultra-violet/visible and near  
28 infrared part of the spectrum. The retrieval is based on the Differential Optical Absorption  
29 Spectroscopy (DOAS; Platt and Stutz, 2008) method using a 425 to 497 nm wavelength  
30 window (Richter et al., 2011) and the reference sector approach (e.g., Richter and Burrows  
31 2002; Martin et al. 2002) applied by IUP-Bremen. Uncertainties in NO<sub>2</sub> satellite retrievals are  
32 large and depend on the region and season. The largest errors are usually found in winter at mid

1 and high latitudes, in regions affected by the Polar vortex due to the nature of the reference  
2 sector approach. As a rough estimate, systematic uncertainties in regions with strong pollution  
3 are on the order of  $\pm 20\text{-}30\%$ . To allow a meaningful comparison to GOME-2 data, the model  
4 data are vertically integrated to TRCNO<sub>2</sub>, interpolated to satellite observation time and then  
5 sampled to match the location of cloud free satellite data. The latter have been gridded to match  
6 the model resolution. Finally, monthly averages of the daily GOME-2 and resulting model data  
7 are calculated in order to reduce any noise. Maps of TRCNO<sub>2</sub> and timeseries for selected areas  
8 (see Table S6) are used for the validation.

9 Tropospheric NO<sub>2</sub> profiles are validated using ground-based multi-axis (MAX-) DOAS  
10 measurements performed in the Beijing city centre (39.98°N, 116.38°E). The period covered  
11 by these observations was from July 2008 to April 2009 but only data until December 2008 are  
12 included here. The retrieval tool and corresponding settings are extensively described in  
13 Hendrick et al. (2014). In brief, measured off-axis and zenith scattered light spectra are analysed  
14 using the DOAS method, providing O<sub>4</sub> (oxygen dimer) and NO<sub>2</sub> slant column densities (SCDs).  
15 In a second step, aerosol extinction coefficient and then NO<sub>2</sub> vertical profiles are retrieved for  
16 each MAX-DOAS scan by applying the OEM (Optimal Estimation Method)-based profiling  
17 algorithm bePRO to the corresponding sets of measured O<sub>4</sub> and NO<sub>2</sub> SCs, respectively. The  
18 retrieval of aerosol vertical profiles is needed since the light path length through the atmosphere  
19 (and thus the measured NO<sub>2</sub> SCDs) strongly depends on the aerosol content. The examination  
20 of the averaging kernels shows that the MAX-DOAS measurements are sensitive to the NO<sub>2</sub>  
21 vertical distribution up to  $\sim 1\text{km}$  altitude (see Hendrick et al., 2014). The validation  
22 methodology is essentially the same as for the NDACC FTIR CO.

23

1 **2 Extra tables**

2 Table S1: Main differences in CIFS-AN and REAN setup

	<b>CIFS-AN</b>	<b>REAN</b>
<b>Model</b>	C-IFS CB05	MOZART
<b>Chemistry</b>	In built chemistry. Tropospheric chemistry scheme. Stratospheric ozone parametrization.	CTM coupled to IFS. Tropospheric and stratospheric chemistry scheme.
<b>Assimilated CO data</b>	MOPITT TCCO	MOPITT TCCO IASI TCCO from Apr - Oct 2008
<b>Assimilated O<sub>3</sub> data</b>	MIPAS, MLS, OMI, SCIAMACHY, SBUV/2	MLS, OMI, SCIAMACHY, SBUV/2
<b>Assimilated NO<sub>2</sub> data</b>	OMI TRCNO2	SCIAMACHY TRCNO2
<b>Data assimilation</b>	NO <sub>2</sub> control variable Modified vertical correlations of O <sub>3</sub> background errors New CO background errors	Nitrogen Oxides (NO <sub>x</sub> ) control variable
<b>Fire emissions</b>	GFAS v1.0	GFED 3
<b>Anthropogenic emissions</b>	MACCITY with enhancement factors of traffic CO over North America and Europe following Stein et al. (2014)	MACCITY

3

4

5

1 Table S2: List of NDACC FTIR stations used for validation in this paper

<b>Station</b>	<b>Region</b>	<b>PI</b>	<b>Latitude, Longitude [°,°]</b>	<b>Altitude [m]</b>
Eureka	Canada	UT	80.0, -86.2	610
Jungfrauoch	Switzerland	ULG	46.5, 8.0	3580
Izaña	Tenerife	FZK	28.3, -16.5	370
Lauder	New Zealand	NIWA	-45.0 169.7	370

2

3

4 Table S3: List of GAW CO stations used for validation in this paper

<b>Station</b>	<b>Latitude, Longitude [°,°]</b>
Alert	82.5, -62.5
Mace Head	53.3, -9.9
Key Biscayne	25.7, -80.2
Ascencion Island	-7.9, -14.4
Samoa	-14.2, -170.6
South Pole	-90.0, -24.8

5

6

1 Table S4: GAW stations used for the validation of surface O<sub>3</sub> data

Station	GAW id	Model Level	Latitude [°]	Longitude [°]	region
1	alt	60	82.45	-62.52	Arctic
2	sum	57	72.57	-38.48	Arctic
3	brw	59	71.32	-156.61	Arctic
4	pal	55	67.97	24.12	Arctic
5	vdl	59	64.25	19.76	Arctic
6	ice	60	63.4	-20.28	Arctic
7	wes	60	54.93	8.32	NH-ML
8	zgt	60	54.43	12.73	NH-ML
9	mhd	60	53.33	-9.90	NH-ML
10	kmw	60	53.33	6.28	NH-ML
11	ngl	59	53.17	13.03	NH-ML
12	lgb	60	52.8	10.77	NH-ML
13	est	60	51.67	-110.2	NH-ML
14	bra	60	50.2	-104.71	NH-ML
15	cps	60	49.82	-74.98	NH-ML
16	ela	60	49.67	-93.72	NH-ML
17	ssl	52	47.92	7.92	NH-ML
18	sat	60	48.78	123.13	NH-ML
19	zsf	48	47.42	10.98	NH-ML
20	rig	59	47.06	8.45	NH-ML
21	snb	48	47.05	12.95	NH-ML
22	alg	57	47.03	-84.38	NH-ML
23	pay	60	46.82	6.95	NH-ML
24	ifj	47	46.55	7.99	NH-ML
25	zrn	55	46.43	15.00	NH-ML
26	kvv	50	46.3	14.53	NH-ML
27	kvk	57	46.12	15.1	NH-ML
28	prs	46	45.93	7.7	NH-ML
29	puy	51	45.77	2.97	NH-ML
30	irb	58	45.57	14.87	NH-ML
31	kej	58	44.43	-65.2	NH-ML
32	egb	60	44.23	-79.78	NH-ML
33	cmn	47	44.18	10.7	NH-ML
34	pdm	47	42.94	0.14	NH-ML
35	beo	47	42.18	23.59	NH-ML
36	thd	59	41.05	-124.15	NH-ML
37	nwr	52	40.04	-105.54	NH-ML
38	ryo	57	39.03	141.82	NH-ML
39	glh	57	36.07	14.21	NH-ML
40	tkb	60	36.05	140.13	NH-ML
41	bmw	59	32.27	-64.88	Tropics
42	izo	46	28.3	-16.5	Tropics
43	pyr	48	27.96	86.81	Tropics
44	yon	60	24.47	123.02	Tropics
45	mnm	60	24.28	153.98	Tropics
46	ask	48	23.27	5.63	Tropics
47	mlo	43	19.54	-155.58	Tropics
48	cvo	60	16.85	-24.87	Tropics
49	rpb	58	13.17	-59.46	Tropics
50	smo	58	-14.23	-170.56	Tropics
51	cpt	57	-34.35	18.48	SH-ML
52	cgo	58	-40.68	144.68	SH-ML
53	bhd	60	-41.41	174.87	SH-ML
54	ldr	60	-45.04	169.68	SH-ML
55	ush	60	-54.83	-68.3	SH-ML
56	syo	60	-69	39.58	Antarctica
57	nmv	60	-70.65	-8.25	Antarctica
58	dcc	59	-75.1	123.33	Antarctica
59	arh	58	-77.8	166.78	Antarctica
60	spo	58	-90	-24.8	Antarctica

1

2 Table S5: Ozonesonde sites used for the validation in various regions

Region	Area S/W/N/E	Stations (Number of observations)
Arctic:	60/-180/90/180	Alert (52), Eureka (83), Keflavik (8), Lerwick (49), Ny-Åalesund (77), Resolute (63), Scoresbysund (54), Sodankylä (63), Summit (81), Thule (15)
North America:	30/-160/60/-50	Boulder (65), Bratts Lake (61), Churchill (61), Egbert (29), Goose Bay (47), Kelowna (72), Narragansett (7), Stony Plain (77), Trinidad Head (35), Wallops (51), Yarmouth (61)
Europe	35/-20/60/40	Ankara (23), Barajas (52), De Bilt (57), Hohenpeissenberg (126), Legionowo (48), Lindenberg (52), Observatoire de Haute-Provence (47), Payerne (158), Prague (49), Uccle (149), Valentia Observatory (49)
East Asia	15/100/60/150	Hong Kong Observatory (49), Naha (37), Sapporo (42), Tateno Tsukuba (49)
Tropics	25/-180/25/180	Alajuela (48), Ascension Island (32), Hanoi (22), Hilo (49), Kuala Lumpur (24), Nairobi (44), Natal (48), Paramaribo (35), Poona (13), Reunion (37), Samoa (33), San Cristobal (28), Suva (28), Thiruvananthapuram (12), Watukosek (20)
Antarctic	-90/-180/-60/180	Davis (24), Dumont d'Urville (38), Maitri (9), Marambio (66), McMurdo (18), Neumayer (72), South Pole (65), Syowa (41)

3

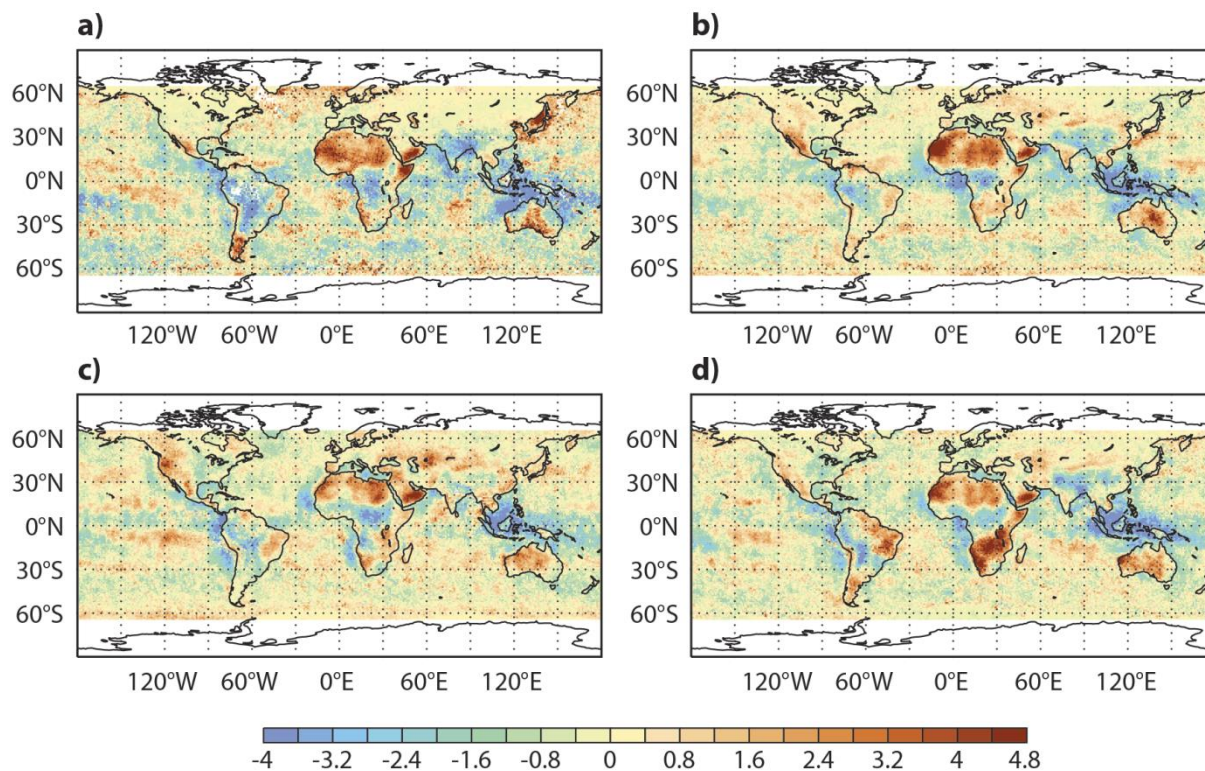
4

5 Table S6: Areas used for the validation against GOME-2 NO<sub>2</sub> retrievals

Area	Area S/W/N/E [°]
East-Asia	20/100/45/145
Europe	35/-15/70/35
Eastern US	30/-120/45/-65
South-Africa	-20/15/0/45

6

1 **3 Extra figures**



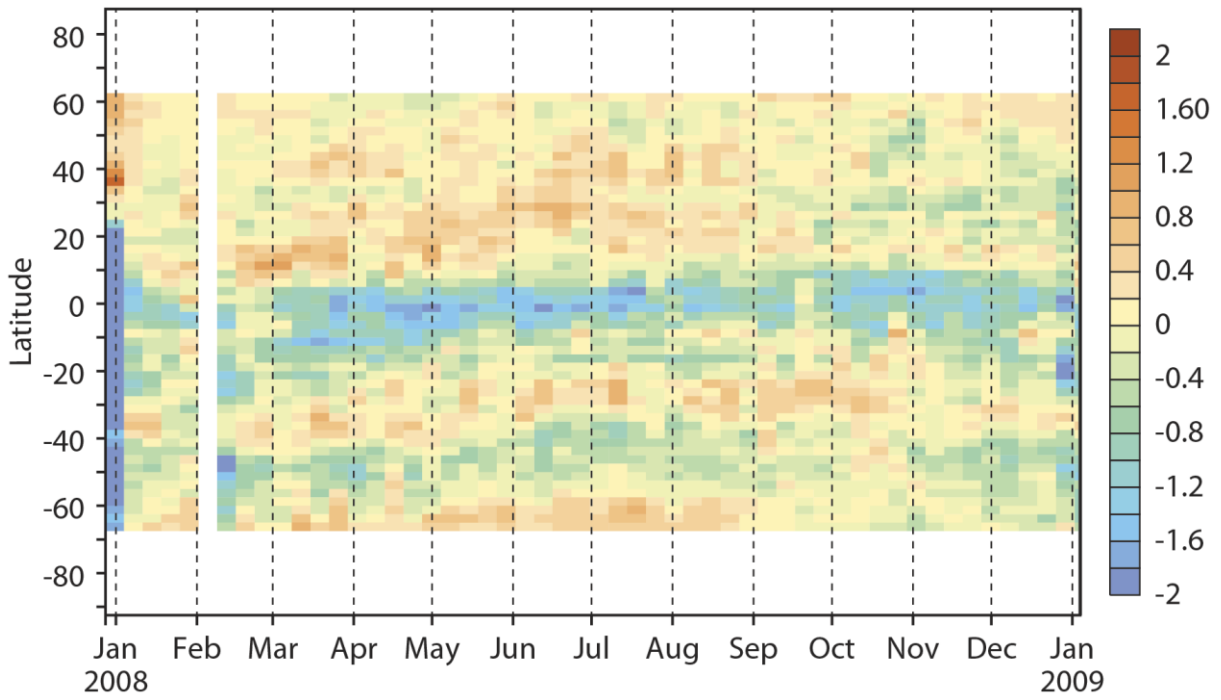
2

3 Figure S1: TCCO analysis increment (analysis minus forecast) in % from CIFS-AN averaged  
4 over (a) JF, (b) MAM, (c) JJA and (d) SON 2008. Red indicates positive values, blue negative  
5 values.

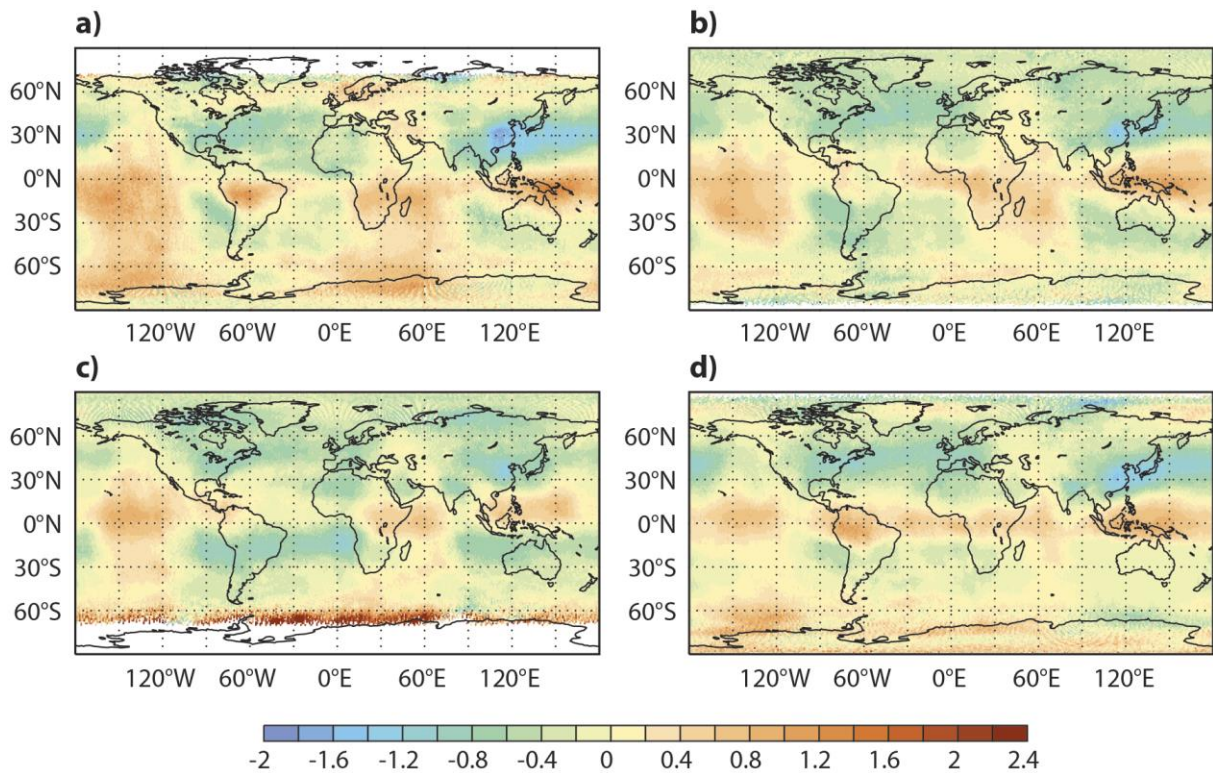
6

7

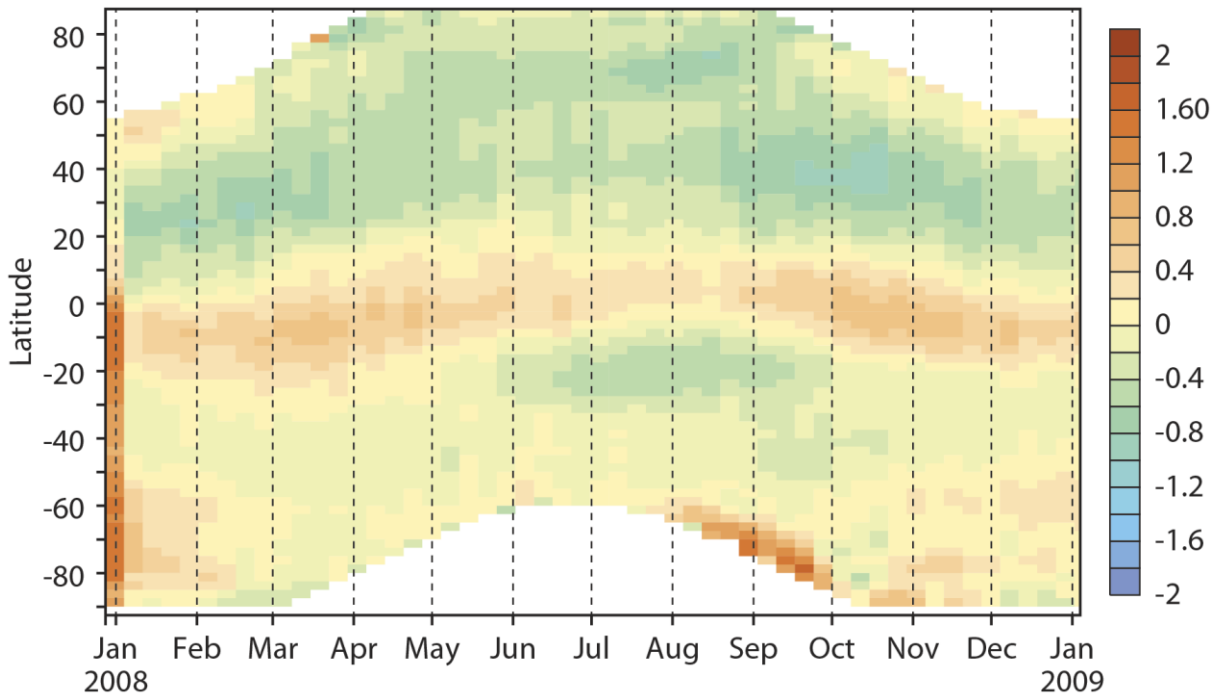
8



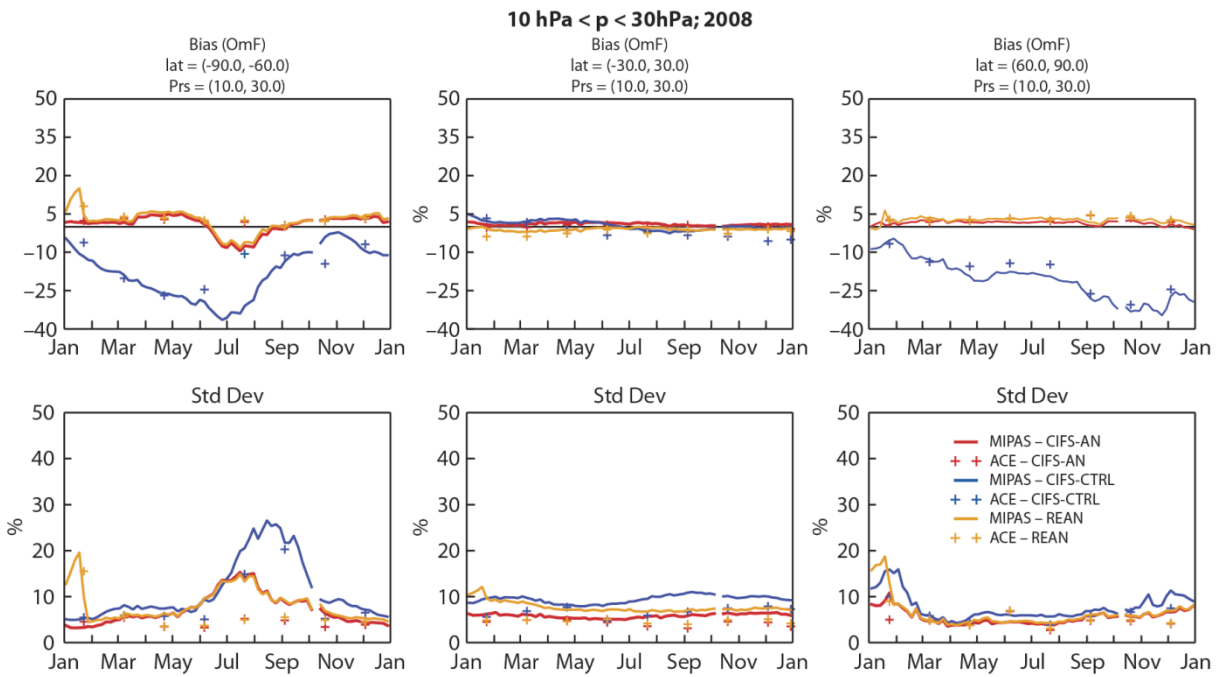
1  
 2 Figure S2: Timeseries of weekly averaged zonal mean MOPITT TCCO analysis increment  
 3 (analysis minus forecast) in % for 2008. Red indicates positive values, blue negative values.



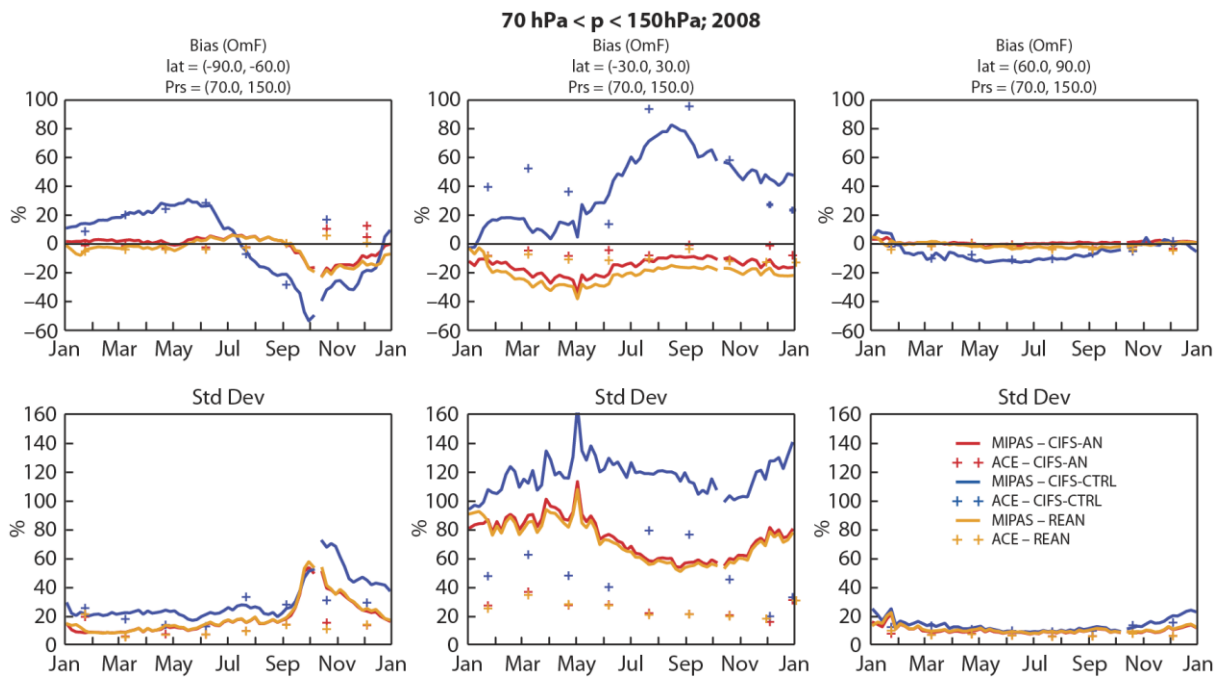
4  
 5 Figure S3: TCO3 analysis increment (analysis minus forecast) in % from CIFS-AN averaged  
 6 over (a) JF, (b) MAM, (c) JJA and (d) SON 2008. Red indicates positive values, blue negative  
 7 values.



1  
 2 Figure S4: Timeseries of weekly averaged zonal mean OMI TCO3 analysis increment (analysis  
 3 minus forecast) in % for 2008. Red indicates positive values, blue negative values.



4  
 5 Figure S5: As in Figure 13 but for the pressure range between 10 and 30 hPa.  
 6



1

2 Figure S6: As in Figure 13 but for the pressure range between 70 and 150 hPa.

3

4 **4 Extra references**

5 Martin, R. V., Chance, K., Jacob, D.J., Kurosu, T.P., Spurr, R.J.D., Bucsela, E., Gleason, J.F.,  
 6 Palmer, P.I., Bey, I., Fiore, A.M., Li, Q., Yantosca, R.M., and Koelemeijer, R.B.A: An  
 7 improved retrieval of tropospheric nitrogen dioxide from GOME, *J. Geophys. Res.*, 107(D20),  
 8 4437, doi:10.1029/2001JD001027, 2002.

9 Platt, U. and Stutz, J.: *Differential Optical Absorption Spectroscopy, Physics of Earth and Space*  
 10 *Environments*, Springer, Berlin, Germany, 2008.

11 Richter, A. and Burrows, J.P.: Tropospheric NO<sub>2</sub> from GOME Measurements, *Adv. Space*  
 12 *Res.*, 29(11),1673-1683, 2002.

13

14